Supporting Information

Burney and Ramanathan 10.1073/pnas.1317275111

SI Text

Model Details. Our model includes state fixed effects (S_i in Eq. **1**) to account for time-invariant differences across the region (e.g., soil type), and state-specific linear and quadratic time trends [$f(t)$] to account for divergent evolution of policies, infrastructure, and management over time between states. We do not explicitly include any technology or management variables (e.g., fertilizer application rates, use of high-yielding varieties, irrigation coverage, and so forth) in any of the models because these changes are captured to some extent in the state-specific time trends. The inclusion of the linear time term effectively detrends the data so that we are not simply correlating increasing quantities (yield, temperature, emissions, and so forth). The inclusion of the quadratic term allows for the possibility that other nonclimate, nonpollution factors may contribute to a leveling-off of yields. Because the dependent variable (Y_{it}) is logged, we can interpret results in terms of percent changes in yield.

Our model includes both climate and pollution variables: T and P, the average growing season temperature and precipitation, as well as T^2 and P^2, the average growing season temperature-squared and precipitation-squared. Inclusion of these squared terms to some degree accounts for extreme temperature and precipitation events and also ensures that our model accounts for weather variations across sites, and not just within sites (1). We standardize T and P by subtracting their means and dividing by their standard deviations (SDs). This approach allows us to interpret the regression coefficients in terms of SDs [i.e., a +1 SD change in T results in a $(\beta_T + 2 * \beta_{T^2}) * 100\%$ change in Y]. The other variables used are: $ln(SO_2)$, average sulfur dioxide emissions (kg m^{-2} s^{-1}); $ln(BC)$, the average BC emissions (kg m^{-2} s^{-1}); $ln(NMVOC)$, the average emissions of nonmethane volatile organic compounds (kg m^{-2} s^{-1}); $ln(NOx)$, the average emissions of nitrogen oxides (kg m^{-2} s^{-1}); and the ratio $ln(NMVOC)$:$ln(NOx)$. The use of logged emissions variables allows for the interpretation of regression coefficients in terms of elasticities; that is, a 1% change in sulfur dioxide emissions leads to a β_{SO_2}% change in yield, and so forth. The physical meaning of the pollution variables (including physical rationale for the logged form) is discussed in greater detail below; sources for all of the above-mentioned data can be found in *Materials and Methods*. As described in *Materials and Methods*, emissions are aggregated over crop area and growing season (for either wheat or rice) to the state-year from monthly gridded datasets.

To calculate the impacts of climate and pollution on yields, we calculated the percent change between predicted values from our main model and predicted values from a baseline scenario. (RYC is calculated using average 2006–2010 values for both model and baseline to avoid influence of fluctuations.) The baseline scenario is counterfactual: it includes only historical technology trends and effectively holds T, P, and aerosol and ozone precursor emissions at 1980 levels (average 1980–1981 levels, to avoid having results influenced by endpoints). These results are presented in Fig. 3. Error bars (90% confidence) are constructed by bootstrap resampling the model 1,000 times and selecting the 5th–95th percentile range. To calculate overall impacts, we summed the state-wide percent changes weighted by area (e.g., totals in Fig. 3) or production (numbers given in main text).

Emissions Variables, Aerosols, and Tropospheric Ozone Chemistry. ***Aerosols.*** Our models give a more complete accounting than previous work (2, 3) of the impacts of short-lived climate forcers on surface radiation by including gridded emissions of sulfur dioxide (SO_2) and black carbon (BC) as markers for surface radiation changes. We include SO_2 as a proxy for sulfate aerosols, because it is the main anthropogenic precursor to sulfates (atmospheric sulfate ions are formed by photochemical oxidation of SO_2 followed by gas-to-particle conversion). BC is a by-product of biomass and fossil fuel combustion (especially diesel); it can be found in the atmosphere in pure (BC) form or in various mixtures with organic carbon (OC) compounds and sulfates. We do not include OC here as it usually appears as Brown Carbon (BrC), the radiative properties of which vary (4).

Ozone precursors. Tropospheric ozone (O_3) forms when ozone precursor compounds react in the presence of sunlight. Formation is highly localized and depends on the presence of both volatile organic compounds (VOCs) or carbon monoxide (CO) and nitrogen oxides ($NOx = NO + NO_2$). (We use VOCs for the remainder of this discussion, although as noted CO can substitute for a VOC in the initial reaction. See below for alternate ozone specifications.) Formation is triggered when a VOC reacts with OH in the atmosphere to form a peroxy radical. These radicals (the hydroxyl, HO_2, is the simplest of the family, represented in general by RO_2) then combine with NO to produce NO_2. At lower NOx concentrations, in the presence of sunlight, NO_2 is photolyzed, providing the extra O that combines with O_2 to form ozone. At high NOx concentrations, NO conversely titrates ozone out of the atmosphere, pulling overall concentrations down. The determinant of these two NOx regimes is the ratio of summed VOCs (weighted by reactivity) to NOx (5).

Our model attempts to account for the potential existence of both high- and low-NOx emissions areas across the study region and represent in a heuristic way some of the above chemistry by including $ln(NOx)$, $ln(NMVOC)$, and the ratio of $ln(NMVOC)$:$ln(NOx)$ (unweighted) in the regression. [Note: VOCs typically include methane, a greenhouse gas that has increased tremendously at global levels over the past decades, but is not usually part of local/regional smog events. It has a fairly uniform global distribution, a longer lifetime than many SLCPs, and is less reactive than many other VOCs. Furthermore, methane is produced during rice cultivation, making it endogenous. We therefore only use NMVOCs (nonmethane VOCs) in this analysis.] At high NOx concentrations, ozone formation is more sensitive to NMVOCs in general (the reaction is NMVOC-limited, and increases in NOx may result in net titration of O_3); at lower NOx concentrations, increases in either NOx or NMVOCs should lead to the formation of ozone (and a decrease in yields). However, the NMVOC:NOx ratio determines the limiting precursor at any given VOC and NOx level. The likelihood of high-NOx regimes in the region is indicated by modeling studies (6, 7), and we find evidence of both NOx regimes in our analysis, as shown in Figs. 2 and 4 and discussed in the main text. (We also conducted the same analysis with different ozone precursor specifications; see below.)

To further inform our model specification, we examined the existing historical data on tropospheric ozone and ozone precursor concentrations in Europe (Fig. 2). Using the European Environment Agency's AirBase database (8), we found the sites and years with valid annual concentration measurements of both ozone and ozone precursors. We then examined the functional relationship between ozone, NOx, total VOCs, and VOC:NOx using this restricted dataset ($n = 57$ site years). The fit between O_3 and the logarithm of precursor concentrations (for both NOx and VOCs independently, and for the ratio term) was much better than the linear fit. Nevertheless, one can see that, for these sites, an empirical NOx threshold for low- and high-NOx

regimes can be determined (~30 μg NO_2/m^3): in the low-NOx regime, O_3 concentrations increase slightly or remain flat with increasing NOx; in the high-NOx regime, O_3 concentrations drop dramatically with increasing NOx (ozone-titrating). We divided the data into low and high NOx to examine the O_3-NOx-VOC relationship in these two regimes. [Note: Most of these sites are urban and are therefore likely in the high NOx regime (i.e., ozone-titrating). This can be seen in the ratio of observations above and below the high-NOx threshold.]

We looked at the equation: $O_3 \sim ln(NOx) + ln(VOC) + [ln(VOC):ln(NOx)]$ for high- and low-NOx regimes. At low-NOx concentrations, both NOx and VOCs are statistically significant predictors of ozone concentrations, and the coefficients for $ln(NOx)$ and the $ln(VOC):ln(NOx)$ ratio are positive. For high NOx concentrations, only NOx is a statistically significant predictor of ozone concentrations, with a negative coefficient. (For the full sample, the coefficients mimic the high-NOx subsample, but with a lower R^2 value, which makes sense given the urban location of most sites in the sample.)

In our analysis we used estimated emissions in lieu of concentrations, because no long-term records of ozone and ozone precursor concentrations exist for India. This analysis therefore assumes that concentrations are proportional to emissions; future work should probe this relationship directly. We also consider only total NMVOC emissions, without accounting for their relative reactivity.

Alternative Model Specifications. ***Consequences of an emissions-based approach.*** As discussed above, emissions are related—but not equivalent—to concentrations, and it is concentrations of BC and ozone that determine radiation changes and plant toxicity exposure, respectively. Using emissions variables (which are themselves estimates constructed from bottom-up technology surveys) as proxies for concentrations may result in either overestimation (by not accounting for deposition, precipitation, and so forth) or underestimation (because of undercounting in emissions inventories) of impacts. Once a reasonable time series of ozone and precursor concentrations exists, the relationship between SLCP emissions, direct and diffuse radiation fractions, and ozone concentrations can be more fully explored. Future research on crop yield impacts will likely use a two-step process, whereby emissions are related to radiation and ozone, which are then related to yields (e.g., a two-stage least squares estimation, not a dose–response estimate).

Climate and pollution interconnectedness. One of the main difficulties in using panel regression analysis to tease out the impacts of SLCPs on yields is the interconnected nature of emissions and climate variables. As mentioned in the main text, SLCPs have their own independent impacts directly on plant growth (ozone) and via surface radiation changes (aerosols); they also impact regional and global climate, which is then in turn reflected in temperature, precipitation, and radiation changes. Beyond the aerosol indirect and semidirect effects, there are additional interactions among the predictor variables that are not addressed in this study. For example: the rate of formation of tropospheric ozone depends on temperature and radiation, as well as the emission of ozone precursors; the presence of tropospheric ozone also alters surface radiation. For simplicity, and because of lack of degrees of freedom, we do not include these secondary interaction terms.

Carbon monoxide and alternate ozone specifications. We conducted our analysis with several variations on the ozone precursor specifications presented in the main text and this *SI Text*. For example, we substituted carbon monoxide for NMVOCs (and an analogous CO:NOx ratio). We also ran a variation using CO+NMVOC. Our results are robust to such changes; the differences on all are within several percentage points (some larger, some smaller). This finding makes sense, as rising CO levels are linked to changes in background ozone but are not thought to contribute as much to the spatial heterogeneity of surface ozone documented over this region. Future research can leverage the increasing network of surface ozone measurements as well as remote sensing of different species. The alternate ozone specifications presented in Fig. S10 are:

i) $ln(NOx)$ only → a simple model using only NOx emissions;
ii) $ln(NMVOC)$ only → models with only NMVOC emissions;
iii) $ln(NOx) + ln(NMVOC):ln(NOx)$ → only NOx and the ratio of NMVOCs to NOx;
iv) $ln(NMVOC):ln(NOx) + ln(BC):ln(SO_2)$ → only the ratios of ozone precursors and the ratio of absorbing to scattering aerosols;
v) $ln(NOx+NMVOC) + ln(NMVOC):ln(NOx) + ln(BC+SO_2) + ln(BC):ln(SO_2)$ → grouped aerosols, grouped precursors, and ratios;
vi) The main model presented in the paper, but with year fixed effects as opposed to linear and quadratic time trends. As expected, the addition of year fixed effects swallows much of the interannual variation in climate.

In addition, models using only NMVOCs, models using non-logged versions of variables, models incorporating CO both individually and as part of the VOC:NOx ratio, and models incorporating organic carbon individually and as part of aerosol totals show very similar results.

Alternative climate and emissions data. As a robustness check, we ran our analysis with alternative climate and emissions datasets. First, we used the temperature and precipitation data from the Climatic Research Unit at East Anglia (half-degree data from CRUTS3.21) (9). Based on findings from previous analyses that showed different crop sensitivity to minimum and maximum temperatures, we also ran our model with T_{min} and T_{max} (10). Finally, we used a new aerosols inventory of BC, organic carbon, and sulfur dioxide (from ref. 11) to check inventory sensitivity. The Lu and Streets inventory (Fig. S11) only begins in 1996; we merged these data with Regional Emissions Inventory in Asia (REAS) data by scaling so that values in 1996 were equal. As shown in Fig. S12, our findings are not sensitive to different climate specifications; the use of the Lu et al. (11) data reduce the magnitude of impacts but maintains the same state-by-state pattern. The overall scale of discrepancy between the inventories (e.g., statewide differences in 1996 data) may explain some of this change.

Carbon dioxide (CO_2) fertilization. We do not explicitly include any measures of CO_2 fertilization in our model. Rather, these effects are aliased into the time trends. Inclusion of CO_2 fertilization directly in our model would be problematic because CO_2 is well-mixed in the atmosphere: because this study uses exposure metrics averaged over crop growing area and growing season, exposure trends are similar over the entire growing area, and effects on each crop should likewise be fairly constant. Nevertheless, it is possible to estimate the average CO_2 impact. Free-air CO_2 enrichment experiments on C_3 crops (including rice and wheat) estimate a 14% increase in crop yields when ambient CO_2 is increased from 367 ppm to 583 ppm, or 0.065% yield change per 1-ppm increase in CO_2 (1, 12). Over the course of this study, average CO_2 concentrations increased from 337 ppm to 390 ppm (keelingcurve.ucsd.edu), which would correspond to a yield increase of just under 3.5%. In certain states, this result offsets the direct temperature and precipitation effects, but does not offset the pollution impacts. Moreover, because CO_2 is emitted in the same combustion processes as aerosols (e.g., coal combustion) and ozone precursor compounds (e.g., transportation), our study points to the further complications in isolating CO_2 impacts on crop yields.

Alternative time controls. Several previous statistical panel studies of climate impacts on yields include year fixed effects (FE), which account for events (like economy-wide shocks) affecting the entire study region in given years. We present results of our model

with the inclusion of year FE in Fig. S10. The trends are similar, but the overall magnitude of SLCP impacts is larger. When year FE are included, climate impacts are predictably smaller given that the year FE consume much of the variation in the climate signal. As this reduction in signal-to-noise can magnify any measurement or data errors, we choose to omit year FE in our main analysis (13).

Kharif-only analysis. We group our analysis by crop under the assumption (informed by chamber and field studies) that the relationship between SLCPs and crop yields should be crop-specific. (That is, even though we include both rabi rice and kharif rice states in our rice analysis, the climate and pollution variables are averaged over the particular state-crop season.) However, to verify that the inclusion of the two main rabi-producing states is not driving the rice results (e.g., because different cultivars are used in the two seasons or because SLCP impacts are expected to be higher during the dry season), we also present kharif-only analysis in Fig. S13. Results are similar, though of a slightly smaller magnitude.

Model Limitations. ***Model training.*** To illustrate that our results are not being driven by particular years or states, we ran our wheat analysis with a subset of data (even years). We then applied those coefficients to the rest of the data (odd years). The results are shown in Fig. S14.

Explanatory power of different variables. The inclusion of state-specific time trends in our model effectively detrends the data; our model thus asks how much of the variation in year-to-year demeaned yields (e.g., Figs. S2 and S3) is explained by the fluctuations in demeaned climate and emissions variables. The relative importance of the time trends can be seen by first regressing the yield, climate, and pollution variables on the state-specific time trends (i.e., explicitly detrending them) and then regressing the yield residuals on the climate and pollution residuals. The coefficients for the explanatory variables will be identical (Frisch–Waugh–Lovell theorem). By comparing these two regressions, we find that the state-specific time trends explain most (about 89%) of the variation in yields. In addition, we can compare a regression of the yield residuals on climate residuals (alone) versus both climate and pollution residuals to compare whether (and how much) the pollution variables add to the model explanatory power. We found that the explanatory power of the full climate-and-pollution model is better than a model with only climate variables and no pollution variables. Table S2 summarizes these results; the detrended relationship is also shown in the inset of Fig. S14.

These results are not surprising. That is, the pollution variables increase the power of the year-to-year predictions, but not by all that much, in part because year-to-year fluctuations aren't that large in the emissions variables (as seen from the time series plots of emissions in Figs. S5–S7). Put another way, the signal-to-noise ratio for the pollution variables is low. This analysis illustrates the need for larger studies over more widely varying pollution regimes or the leveraging of natural experiments that produce greater year-to-year variation in emissions. In addition, a finer-grained look at management practices may help gain leverage on the remaining variation.

Collinearity. In addition to low signal-to-noise for the emissions variables, our analysis is limited because of multicollinearity, or the strong linear correlation of independent variables in a regression analysis (in this case, the emissions variables, which are all fairly monotonically increasing over time) (Figs. S5–S7, S11, and Table S3). The presence of multicollinearity does not undermine the reliability of the model as a whole (e.g., results in Fig. 3), but it affects our ability to distinguish with certainty the individual impact of the correlated variables, as the variances are inflated. It is for this reason that we are unable to quantify with certainty the relative impacts of aerosols versus ozone within SLCP impacts. In general, the antidote to multicollinearity is more data, adding for example, other countries to a dataset or undertaking analysis at a smaller unit of scale. The latter is only a limited option in this case, as relating local emissions to local yield changes would become invalid at a smaller scale (because of shorter-range pollutant transport). However, expanding the analysis to include other regions of the world (as data become available) points to a promising future avenue of research.

1. Lobell DB, Schlenker W, Costa-Roberts J (2011) Climate trends and global crop production since 1980. *Science* 333(6042):616–620.
2. Auffhammer M, Ramanathan V, Vincent JR (2006) Integrated model shows that atmospheric brown clouds and greenhouse gases have reduced rice harvests in India. *Proc Natl Acad Sci USA* 103(52):19668–19672.
3. Auffhammer M, Ramanathan V, Vincent J (2011) Climate change, the monsoon, and rice yield in India. *Clim Change* 111(2):411–424.
4. Chung CE, Ramanathan V, Decremer D (2012) Observationally constrained estimates of carbonaceous aerosol radiative forcing. *Proc Natl Acad Sci USA* 109(29):11624–11629.
5. Sillman S (1999) The relation between ozone, NOx and hydrocarbons in urban and polluted rural environments. *Atmos Environ* 33(12):1821–1845.
6. Van Dingenen R, et al. (2009) The global impact of ozone on agricultural crop yields under current and future air quality legislation. *Atmos Environ* 43(3):604–618.
7. Avnery S, Mauzerall DL, Liu J, Horowitz LW (2011) Global crop yield reductions due to surface ozone exposure: 2. Year 2030 potential crop production losses and economic damage under two scenarios of O_3 pollution. *Atmos Environ* 45(13):2297–2309.
8. European Environment Agency Topic Centre on Air Pollution and Climate Change Mitigation, AirBase, version 6.0. Available at acm.eionet.europa.eu/databases/airbase. Accessed February 25, 2013.
9. Climatic Research Unit, High-Resolution Gridded Climate Datasets (CRU TS3.21). Available at www.cru.uea.ac.uk/cru/data/hrg. Accessed May 5, 2014.
10. Welch JR, et al. (2010) Rice yields in tropical/subtropical Asia exhibit large but opposing sensitivities to minimum and maximum temperatures. *Proc Natl Acad Sci USA* 107(33):14562–14567.
11. Lu Z, Zhang Q, Streets DG (2011) Sulfur dioxide and primary carbonaceous aerosol emissions in China and India, 1996–2010. *Atmos Chem Phys* 11:9839–9864.
12. Ainsworth EA, Long SP (2005) What have we learned from 15 years of free-air CO_2 enrichment (FACE)? A meta-analytic review of the responses of photosynthesis, canopy properties and plant production to rising CO2. *New Phytol* 165(2):351–371.
13. Fisher AC, Hanemann WM, Roberts M, Schlenker W (2012) The economic impacts of climate change: Evidence from agricultural output and random fluctuations in weather. *Am Econ Rev* 102:3749–3760.

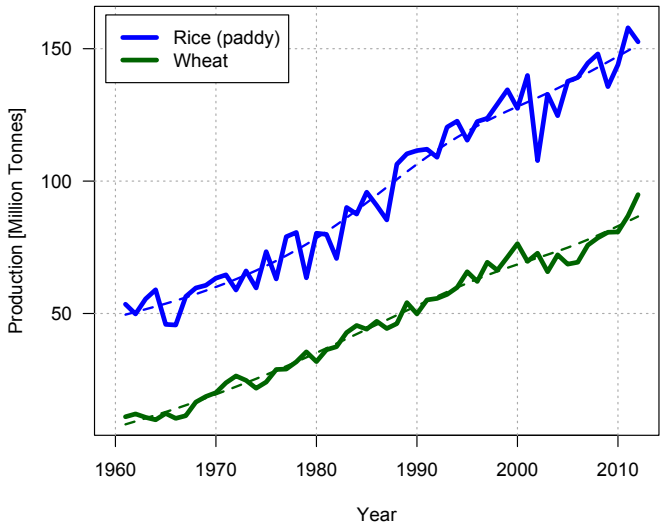

Fig. S1. Historic wheat and rice production in India, 1961–2012.

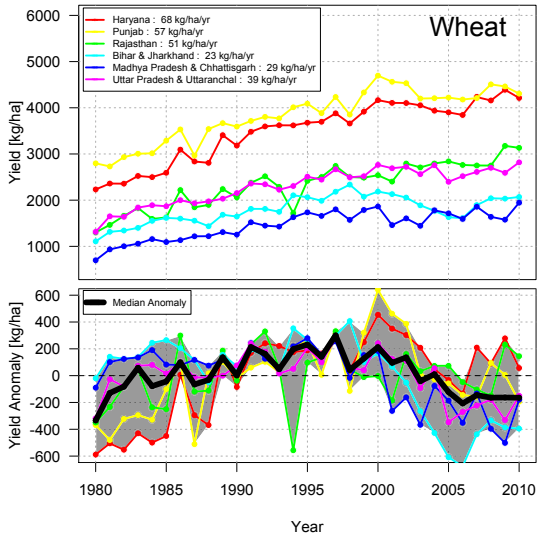

Fig. S2. (*Top*) Wheat yields in the main wheat-producing states in India. (*Bottom*) Detrended wheat yields, showing deviation from fitted state-specific linear trends. Data from IndiaStat.com (1).

1. Datanet India, IndiaStat. Available at www.indiastat.com. Accessed July 17, 2012.

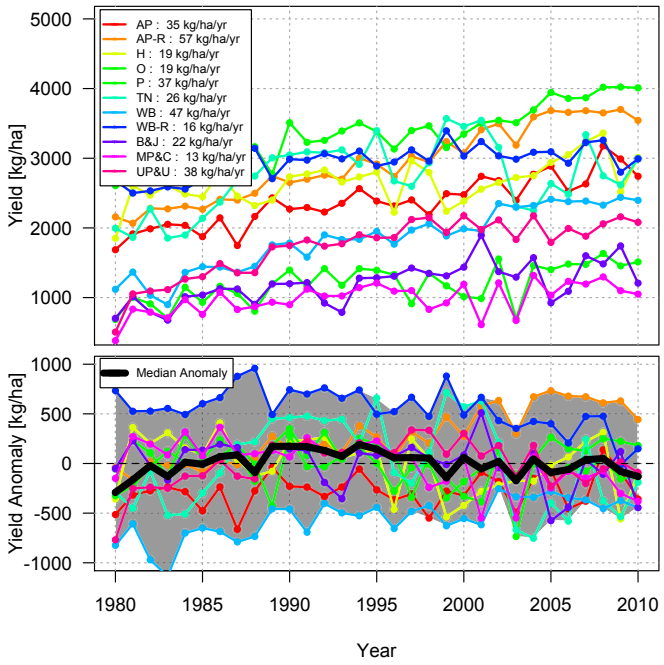

Fig. S3. (*Top*) Rice yields in the main rice-producing states in India. (*Bottom*) Detrended rice yields, showing deviation from fitted state-specific linear trends. Data from IndiaStat.com (1).

1. Datanet India, IndiaStat. Available at www.indiastat.com. Accessed July 17, 2012.

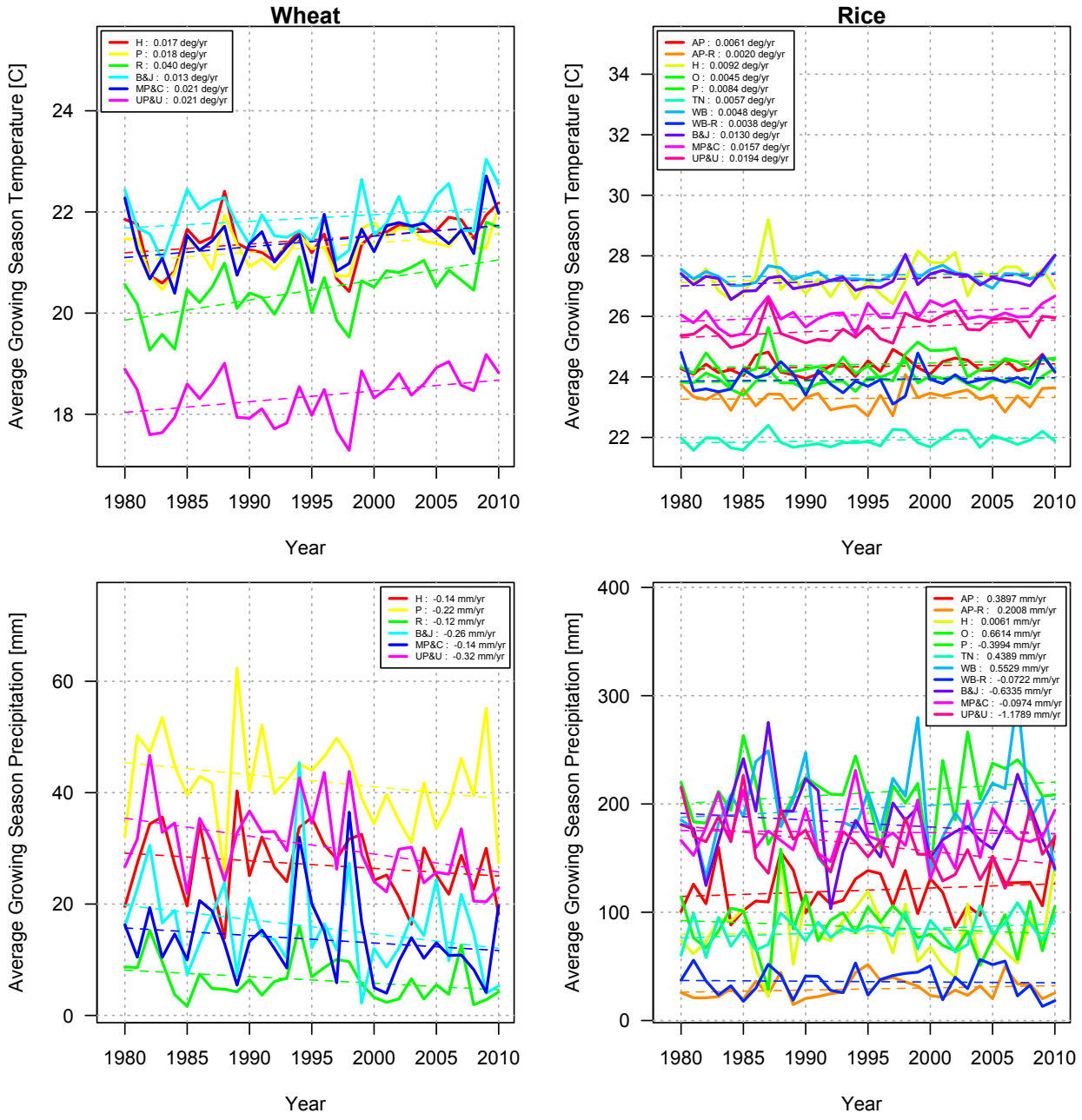

Fig. S4. Growing season temperature and precipitation trends for major rice- and wheat-producing states in India, 1980–2010.

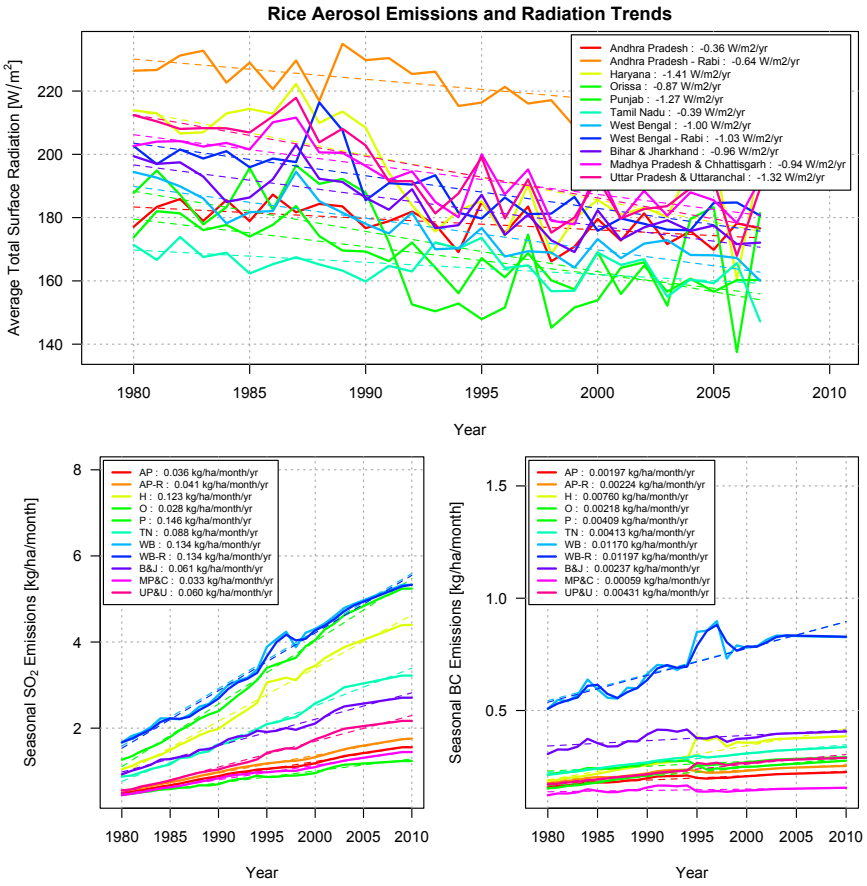

Fig. S5. (*Top*) Trends in total average daily surface radiation over the kharif rice growing season, by state. State-specific linear dimming trends (fitted slopes) shown in the legend. Data from the World Radiation Data Centre (1). (*Bottom*) Emissions of (*Left*) SO_2 and (*Right*) BC by state over the season, with state-specific linear emissions trends (fitted slopes) shown in the legend. Data from the REAS emissions inventory (2).

1. World Radiation Data Center (WRDC), Global Radiation Data. Available at wrdc.mgo.rssi.ru. Accessed June 9, 2011.
2. Ohara T, et al. (2007) An Asian emission inventory of anthropogenic emission sources for the period 1980–2020. *Atmos Chem Phys* 7:4419–4444.

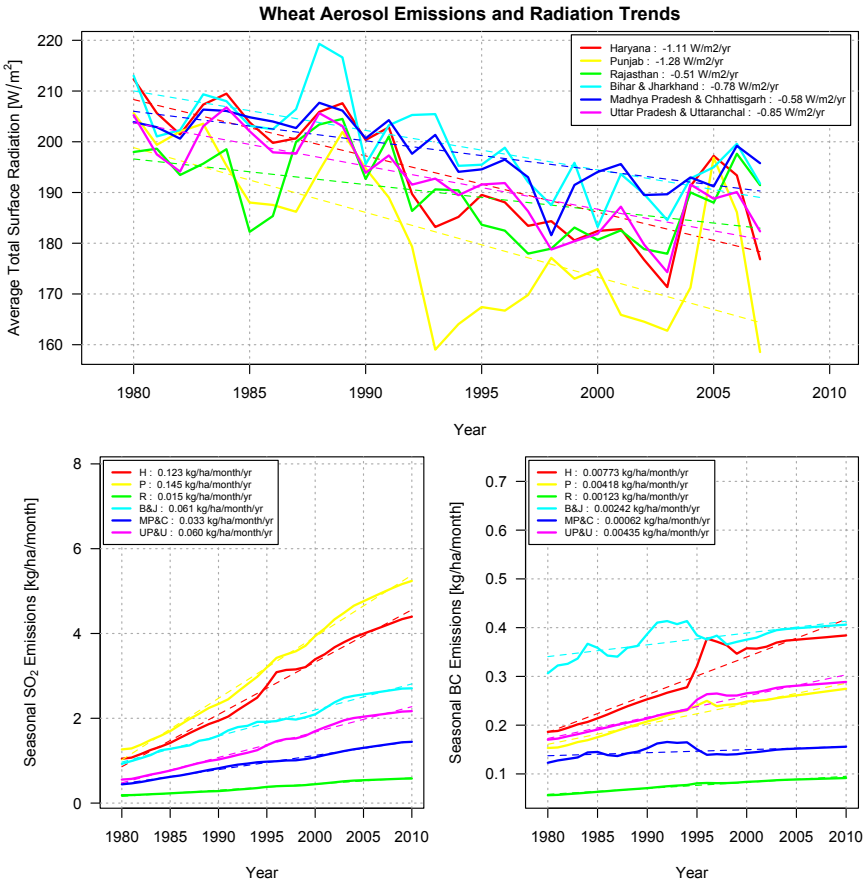

Fig. S6. (*Top*) Trends in total average daily surface radiation over the wheat growing season, by state. State-specific linear dimming trends (fitted slopes) shown in the legend. Data from the World Radiation Data Centre (1). (*Bottom*) Emissions of (*Left*) SO_2 and (*Right*) BC by state over the season, with state-specific linear emissions trends (fitted slopes) shown in the legend. Data from the REAS emissions inventory (2).

1. World Radiation Data Center (WRDC), Global Radiation Data. Available at wrdc.mgo.rssi.ru. Accessed June 9, 2011.
2. Ohara T, et al. (2007) An Asian emission inventory of anthropogenic emission sources for the period 1980–2020. *Atmos Chem Phys* 7:4419–4444.

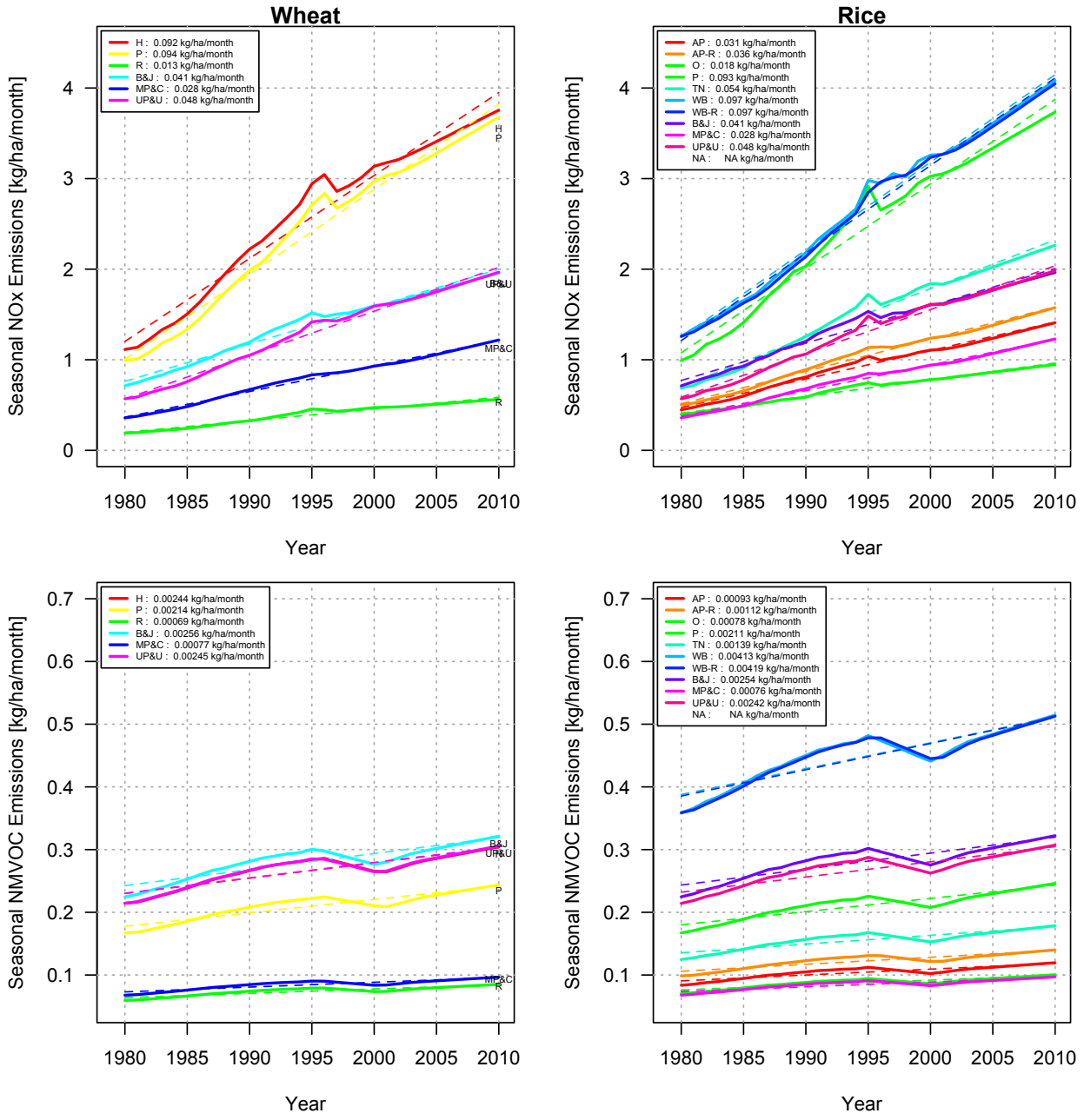

Fig. S7. Trends in NOx and NMVOC emissions for major wheat- and rice-producing states in India, 1980–2010. Data from REAS emissions inventory (1).

1. Ohara T, et al. (2007) An Asian emission inventory of anthropogenic emission sources for the period 1980–2020. *Atmos Chem Phys* 7:4419–4444.

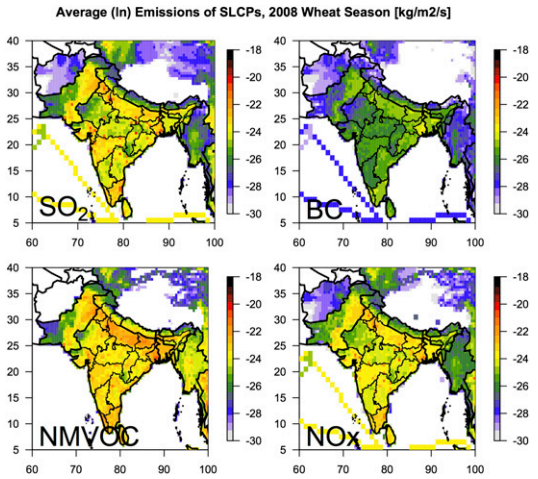

Fig. S8. Average wheat growing season emissions of SO_2, BC, NMVOC, and NOx in 2008. Data from the REAS emissions inventory (1).

1. Ohara T, et al. (2007) An Asian emission inventory of anthropogenic emission sources for the period 1980–2020. *Atmos Chem Phys* 7:4419–4444.

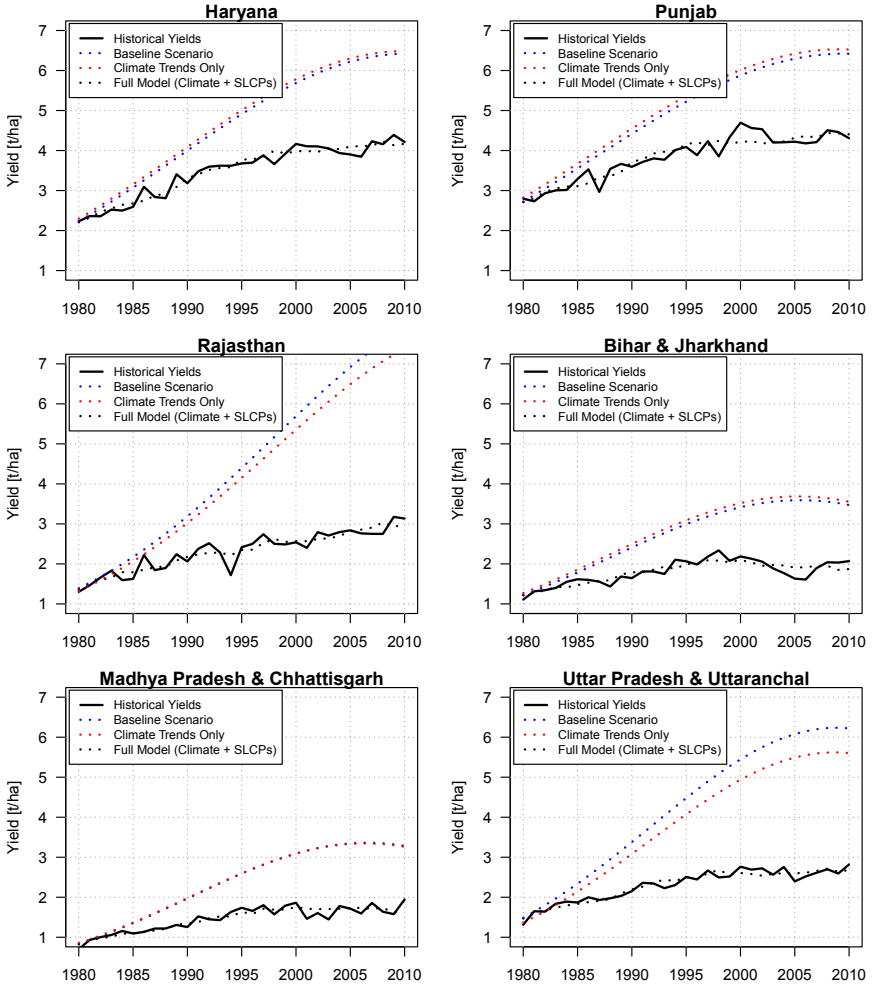

Fig. S9. State-by-state breakdown of impacts of technology/time trends, climate, and pollution for wheat-producing states.

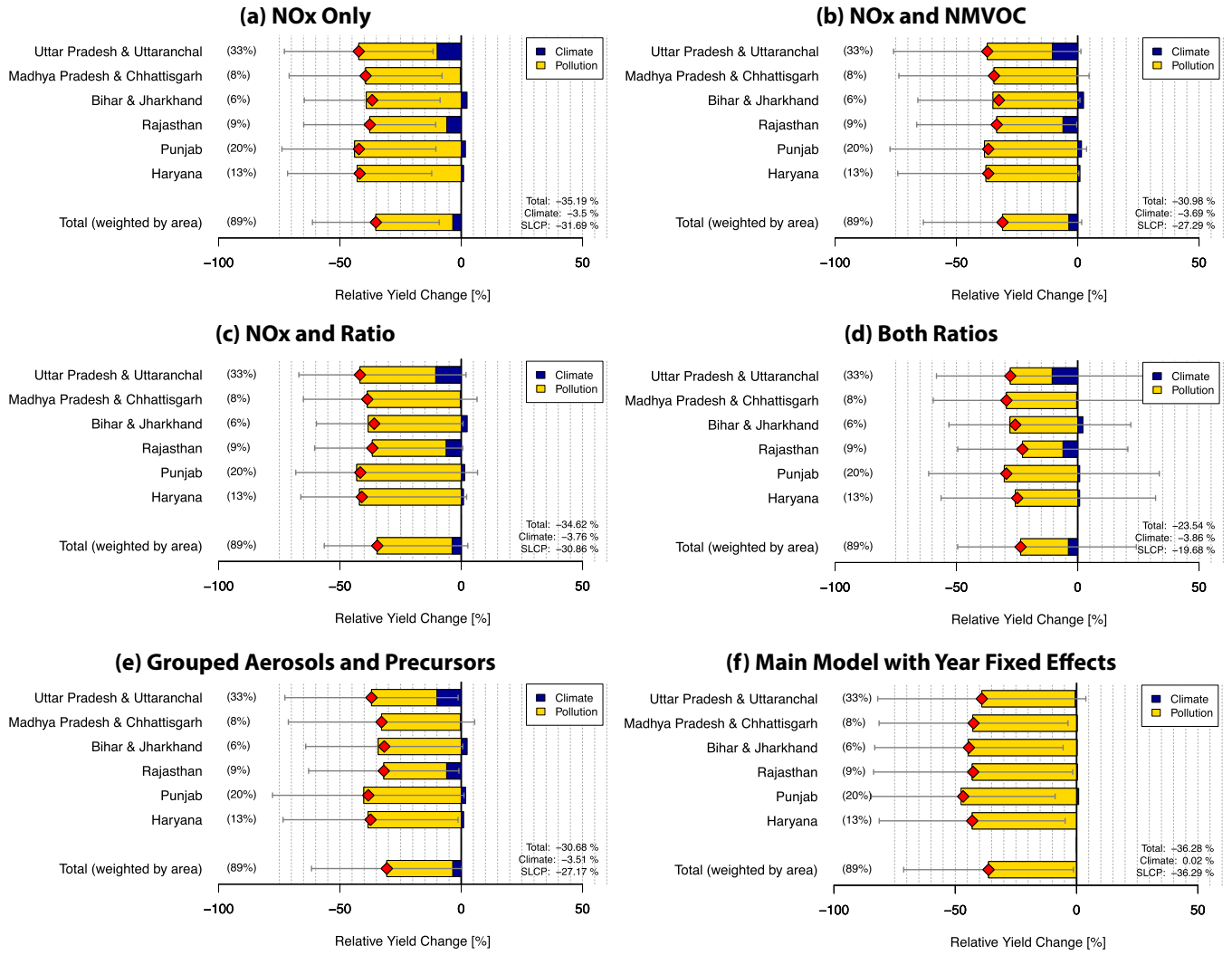

Fig. S10. Alternative model specifications for wheat. These models use different specifications for ozone precursor and aerosol emissions, as shown in the figure legend. Models are described in more detail in *SI Text*.

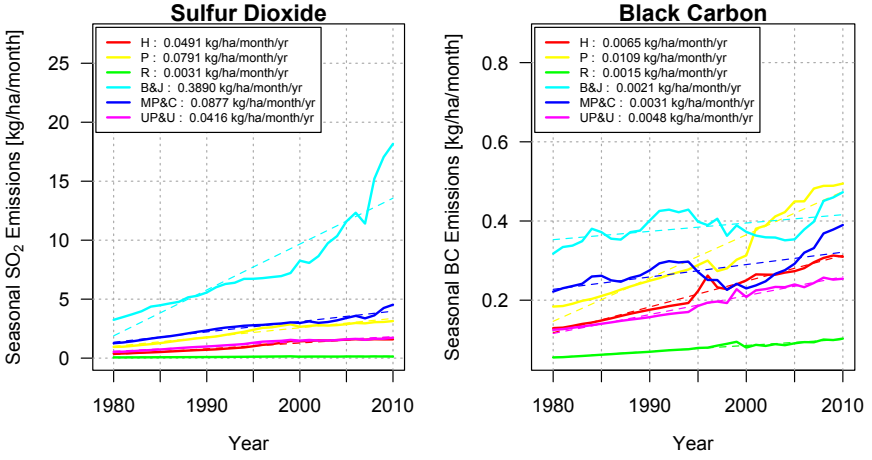

Fig. S11. Emissions trends from Lu and Streets aerosols inventory (1). The inventory begins in 1996; we merged these data with REAS data by scaling so that values in 1996 were equal.

1. Lu Z, Zhang Q, Streets DG (2011) Sulfur dioxide and primary carbonaceous aerosol emissions in China and India, 1996–2010. *Atmos Chem Phys* 11:9839–9864.

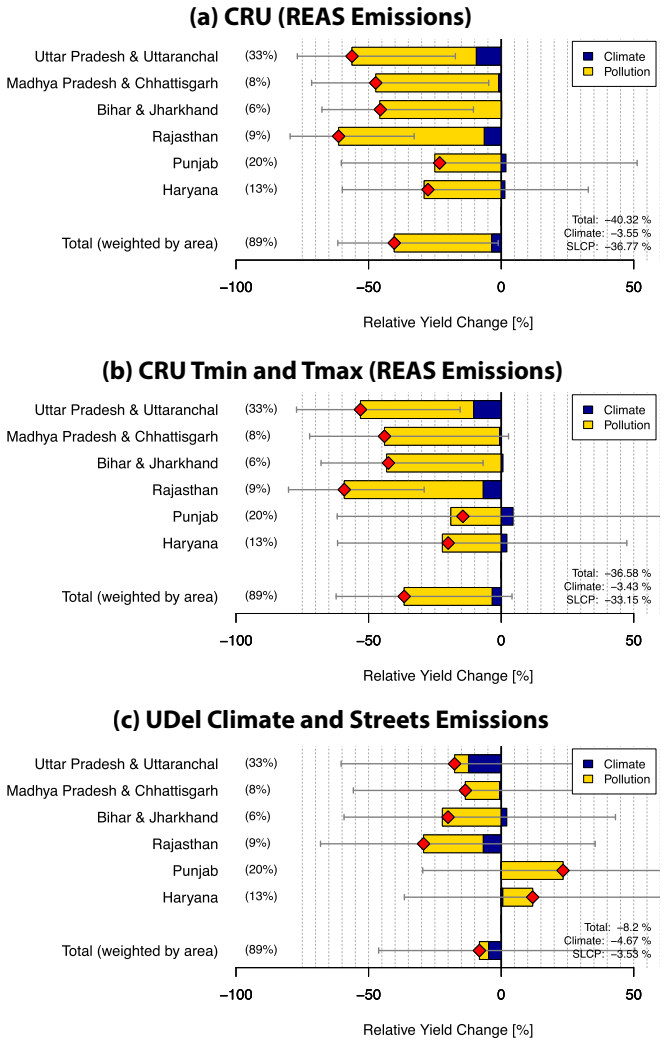

Fig. S12. Analysis with alternative climate and emissions datasets. CRU data are from the Climatic Research Unit at East Anglia; we used half-degree data from CRUTS3.21 (1). The first specification (*A*) replicates the main model presented in the paper, but with CRU data replacing University of Delaware data. The second specification (*B*) uses T_{min} and T_{max}, as recent research has shown that crops are sensitive in different ways to these two quantities (2). The third specification (*C*) uses a different, higher-resolution ($0.1° \times 0.1°$) emissions inventory for the aerosols portion of the model. The Streets inventory of black carbon, organic carbon, and sulfur dioxide (3) begins in 1996; we merged these data with REAS data by scaling so that values in 1996 were equal.

1. Climatic Research Unit, High-Resolution Gridded Climate Datasets (CRU TS3.21). Available at www.cru.uea.ac.uk/cru/data/hrg. Accessed May 5, 2014.
2. Welch JR, et al. (2010) Rice yields in tropical/subtropical Asia exhibit large but opposing sensitivities to minimum and maximum temperatures. *Proc Natl Acad Sci USA* 107(33):14562–14567.
3. Lu Z, Zhang Q, Streets DG (2011) Sulfur dioxide and primary carbonaceous aerosol emissions in China and India, 1996–2010. *Atmos Chem Phys* 11:9839–9864.

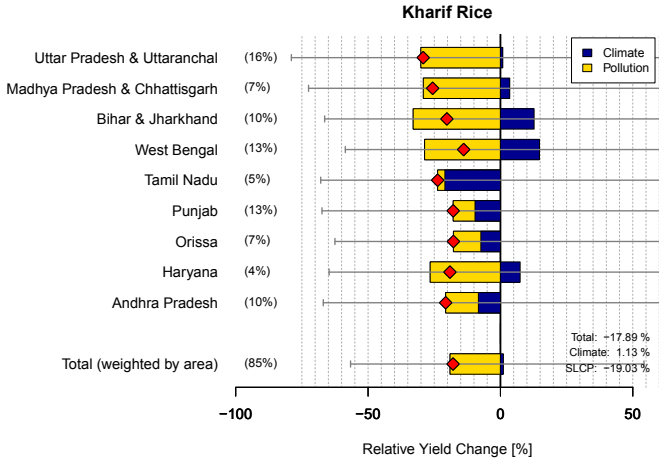

Fig. S13. Main model with only kharif (rainy season) rice.

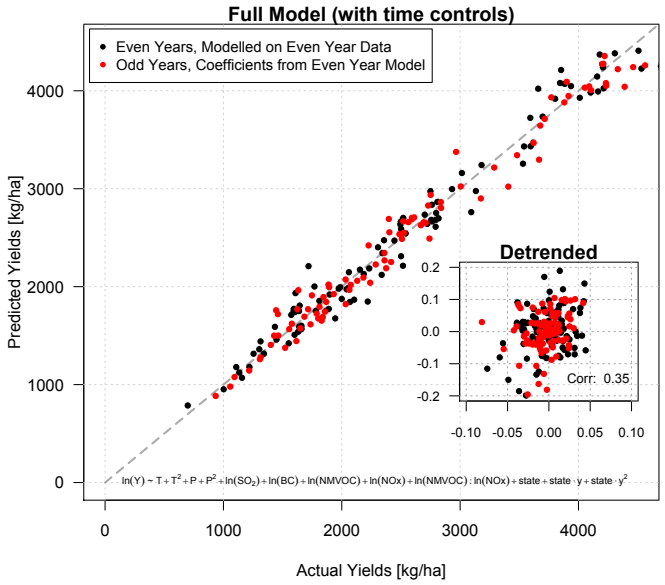

Fig. S14. Even-odd analysis. Main plot shows predicted versus actual wheat yields for model fit to even-year data (black), and predictions (from even-year fit) to odd-year data. *Inset* shows fits from residuals of detrended variables.

Table S1. Regression coefficients for wheat and rice (Eq. 1)

	Wheat	Rice
Variables	ln(Yield)	ln(Yield)
T	−0.051** (0.021)	−0.552 (0.601)
T^2	−0.000 (0.005)	−0.130 (0.492)
P	−0.015 (0.015)	−0.040 (0.026)
P^2	0.002 (0.006)	0.007 (0.017)
ln(BC)	0.247 (0.182)	0.193 (0.332)
ln(SO_2)	−0.756*** (0.238)	−0.562 (0.532)
ln(NOx)	−7.228** (3.511)	0.483 (7.875)
ln(NMVOC)	7.111** (3.294)	0.328 (7.403)
ln(NOx): ln(NMVOC)	162.145** (76.157)	−5.462 (170.982)
Year	0.035*** (0.009)	0.021 (0.016)
Year^2	−0.002*** (0.000)	−0.000 (0.001)
Constant	−168.392** (81.200)	25.634 (185.259)
Observations	186	341
R^2	0.9999	0.9998
rmse	0.0704	0.128

SEs in parentheses; ***$P < 0.01$, **$P < 0.05$, *$P < 0.1$. State-specific intercepts and linear and quadratic time coefficients not shown for brevity. Coefficients for T and T^2, P and P^2, and ozone precursors must be interpreted collectively. For wheat, temperature is statistically significant at 90% ($P = 0.051$), aerosols are significant at 99% ($P = 0.003$), and ozone precursors are significant at 90% ($P = 0.056$). For rice, temperature is statistically significant at 95% ($P = 0.016$), aerosols are not statistically significant, and ozone precursors are significant at 99% ($P = 0.005$).

Table S2. Explanatory power of time trend, climate, and pollution variables

Model	Adjusted R^2	rmse
Full model	0.9687	0.0704
Detrended model (climate and pollution variables)	0.0746	0.0669
Detrended climate-only model	0.0346	0.0683

Table S3. Correlations between state-level variables for wheat analysis

	Year	Temperature	Precipitation	*ln(SO_2)*	*ln(BC)*	*ln(NOx)*	*ln(NMVOC)*
Year	1.0000						
Temperature	0.1110	1.0000					
Precipitation	−0.0970	−0.1952	1.0000				
ln(SO_2)	0.4667	0.2996	0.5766	1.0000			
ln(BC)	0.2485	0.2066	0.4268	0.8532	1.0000		
ln(NOx)	0.4560	0.2285	0.6026	0.9848	0.8256	1.0000	
ln(NMVOC)	0.1407	−0.0536	0.5734	0.7781	0.9054	0.7990	1.0000